JFM RAPIDS
journals.cambridge.org/rapids

The Graetz–Nusselt problem extended to continuum flows with finite slip

A. Sander Haase[1], S. Jonathan Chapman[2], Peichun Amy Tsai[1], Detlef Lohse[3] and Rob G. H. Lammertink[1],†

[1]Soft matter, Fluidics and Interfaces, MESA$^+$ Institute for Nanotechnology, University of Twente, PO Box 217, 7500 AE Enschede, The Netherlands

[2]Mathematical Institute, University of Oxford, 24-29 St Giles, Oxford OX1 3LB, UK

[3]Physics of Fluids, MESA$^+$ Institute for Nanotechnology, University of Twente, PO Box 217, 7500 AE Enschede, The Netherlands

Graetz and Nusselt studied heat transfer between a developed laminar fluid flow and a tube at constant wall temperature. Here, we extend the Graetz–Nusselt problem to dense fluid flows with partial wall slip. Its limits correspond to the classical problems for no-slip and no-shear flow. The amount of heat transfer is expressed by the local Nusselt number Nu_x, which is defined as the ratio of convective to conductive radial heat transfer. In the thermally developing regime, Nu_x scales with the ratio of position $\tilde{x} = x/L$ to Graetz number Gz, i.e. $Nu_x \propto (\tilde{x}/Gz)^{-\beta}$. Here, L is the length of the heated or cooled tube section. The Graetz number Gz corresponds to the ratio of axial advective to radial diffusive heat transport. In the case of no slip, the scaling exponent β equals 1/3. For no-shear flow, $\beta = 1/2$. The results show that for partial slip, where the ratio of slip length b to tube radius R ranges from zero to infinity, β transitions from 1/3 to 1/2 when $10^{-4} < b/R < 10^0$. For partial slip, β is a function of both position and slip length. The developed Nusselt number Nu_∞ for $\tilde{x}/Gz > 0.1$ transitions from 3.66 to 5.78, the classical limits, when $10^{-2} < b/R < 10^2$. A mathematical and physical explanation is provided for the distinct transition points for β and Nu_∞.

Key words: boundary layers, convection, free shear layers

1. Introduction

The classical Graetz–Nusselt problem concerns a fluid of uniform temperature T_0 flowing in an insulated cylindrical tube. The flow is laminar and hydrodynamically

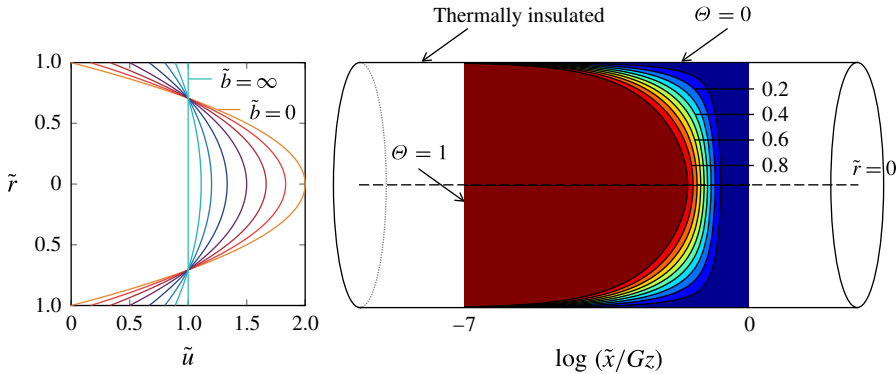† Email address for correspondence: r.g.h.lammertink@utwente.nl

FIGURE 1. The Graetz–Nusselt problem concerns transport of heat between a hydrodynamically fully developed fluid flow with $\Theta = (T_1 - T)/(T_1 - T_0) = 1$ and a tube with a constant wall temperature $\Theta = 0$ for $\tilde{x} > 0$. The velocity profile of the inflowing fluid is a function of the tube radius $\tilde{r}$ and the slip length $\tilde{b}$, where $0 \leqslant \tilde{b} \leqslant \infty$. The profile is parabolic for $\tilde{b} = 0$ and uniform for $\tilde{b} = \infty$. The contour map gives an example of a temperature profile.

fully developed, and has constant physical properties (see figure 1). At $x = 0$ the fluid enters a tube section with a constant wall temperature T_1. Neglecting viscous dissipation and axial heat conduction, Graetz (1882, 1885) and Nusselt (1910) independently found a mathematical solution to this problem, describing the temperature profile for $x > 0$. The problem was solved for both a uniform (Graetz 1882) and a parabolic (Graetz 1885; Nusselt 1910) fluid velocity profile. From the temperature distribution the local heat flux at the wall can be obtained, which is commonly expressed by the local Nusselt number Nu_x, a dimensionless heat transfer coefficient (Eckert & Drake 1972; Bird, Stewart & Lightfoot 2007). The Nusselt number

$$Nu_x = \frac{h_x D}{k}, \tag{1.1}$$

where h_x is the local heat transfer coefficient, $D = 2R$ is the diameter of the tube and k is the thermal conductivity, can be interpreted as the ratio of convective to conductive radial heat transfer (Jakob 1949; Shah & London 1978). The Nusselt number Nu_x is a function of the dimensionless downstream position $\tilde{x} = x/L$, L being the length of the non-insulated section of the tube, and the Graetz number Gz only. The Graetz number is defined as (Jakob 1949; Shah & London 1978)

$$Gz = \frac{u_{av} D^2}{\alpha L} = RePr\frac{D}{L}, \tag{1.2}$$

where u_{av} is the average fluid velocity and α is the thermal diffusivity. It is the product of the Reynolds number $Re = u_{av} D/\nu$, the Prandtl number $Pr = \nu/\alpha$ and the ratio D/L, and can be interpreted as the ratio of axial advective to radial diffusive heat transport.

The temperature profiles found by Graetz and Nusselt involve infinite series in terms of eigenvalues and eigenfunctions. When $\tilde{x}/Gz > 0.1$, the first terms of the series solutions dominate. This results in a developed Nusselt number $Nu_\infty = 3.66$ for parabolic flow and $Nu_\infty = 5.78$ for plug flow (Shah & London 1978). The flow is said to be thermally fully developed. For $\tilde{x}/Gz < 0.01$, when the flow is thermally

developing, and in particular when $x \to 0$, a very large number of terms are required to obtain the Nusselt number with sufficient accuracy. Lévêque (1928) circumvented this problem by assuming that in the entrance region the thermal boundary layer is thin compared with the viscous boundary layer (Eckert & Drake 1972; Shah & London 1978; Bird *et al.* 2007). In that case curvature effects can be neglected. Furthermore, it can be assumed that the bulk extends to infinity, and that the velocity profile is linear. Lévêque showed that

$$Nu_x \propto \left(\frac{\tilde{x}}{Gz} \right)^{-\beta}, \tag{1.3}$$

with $\beta = 1/3$ for a parabolic velocity profile and $\beta = 1/2$ for a uniform velocity profile. Essentially, complete solutions for the Graetz–Nusselt problem found in the literature are a combination of the methods of Graetz and Lévêque (Shah & London 1978).

There are special cases where the no-slip or the no-shear boundary condition does not hold. The effects of slip phenomena encountered in rarefied gas flows, which include velocity and temperature jumps at the tube wall (Eckert & Drake 1972; Karniadakis, Beskok & Aluru 2005), were first investigated by Sparrow & Lin (1962). Both wall slip and temperature jump are a function of the Knudsen number Kn, the ratio of mean free path to tube diameter. Their results show that Nu_∞ decreases with increasing mean free path, which implies increasing wall slip and larger temperature jumps. Barron *et al.* (1997) found that, for a given Graetz number, the Nusselt number becomes larger with increasing slip. Although they explicitly incorporated the temperature jump in the boundary conditions, it was ignored in the calculation of the eigenvalues (Ezquerra Larrodé, Housiadas & Drossinos 2000). It is crucial to account for the temperature jump at the wall for rarefied gas flows, since the effect of this temperature jump is dominant over the influence of wall slip (Ezquerra Larrodé *et al.* 2000; Colin 2011).

In continuum flows, i.e. liquid and gas flows for which $Kn < 10^{-2}$, a temperature jump is not present (Eckert & Drake 1972; Karniadakis *et al.* 2005). Moreover, in most situations the no-slip boundary condition is correct (Eckert & Drake 1972; Lauga, Brenner & Stone 2007). However, with the rise of micro- and nanofluidics it became apparent that the no-slip boundary condition for liquid flows does not always hold (Lauga *et al.* 2007). Intrinsic slip lengths vary from nearly zero (Bocquet & Barrat 2007; Rothstein 2010) to almost infinity (Whitby & Quirke 2007; Majumder, Chopra & Hinds 2011). Here, the slip length is defined by Navier's slip condition (Navier 1823),

$$u_s = -b \left. \frac{\partial u}{\partial r} \right|_{r=R}, \tag{1.4}$$

which states that the liquid velocity at the wall u_s is proportional to the slip length b and the velocity gradient $\partial_r u$ at the wall. This implies that the classical Graetz–Nusselt solutions are not applicable to this type of flow.

In this paper we present numerical and analytical solutions to the Graetz–Nusselt problem for continuum flows with finite slip. The effects of wall slip on both the exponent β and Nu_∞, characteristic for heat transport in the thermally developing and thermally developed regimes, are investigated. The results reveal distinct transition points for β and Nu_∞ when the slip length b goes from zero to infinity. These transition points are explained both mathematically and physically.

2. Mathematical model

2.1. *Heat equation*

A schematic representation of the Graetz–Nusselt problem is provided in figure 1. Here, under the assumptions given in § 1, the governing equation describing stationary heat transport in a cylindrical system can be written as

$$u\frac{\partial T}{\partial x} = \frac{\alpha}{r}\frac{\partial}{\partial r}\left(r\frac{\partial T}{\partial r}\right), \tag{2.1}$$

where $u(r, b)$ describes the velocity profile of the laminar fluid flow in the x-direction. The boundary conditions are $T(0, r) = T_0$ and $T(x, R) = T_1$. At $x = 0$, the flow is hydrodynamically fully developed. Solution of the Navier–Stokes equation for stationary slip flow in the axial direction yields the following expression for the velocity profile:

$$\tilde{u} = \frac{2\left(1 - \tilde{r}^2\right) + 4\tilde{b}}{1 + 4\tilde{b}}, \tag{2.2}$$

where $\tilde{u} = u/u_{av}$, $\tilde{r} = r/R$ and $\tilde{b} = b/R$. Here, $\tilde{u}$ can be interpreted as the sum of the variable velocity $\tilde{u}_v(\tilde{r}, \tilde{b}) = 2(1 - \tilde{r}^2)/(1 + 4\tilde{b})$ and the slip velocity $\tilde{u}_s(\tilde{b}) = 4\tilde{b}/(1 + 4\tilde{b})$. The heat equation can now be non-dimensionalised using $\Theta = (T_1 - T)/(T_1 - T_0)$ and $\tilde{x} = x/L$,

$$\frac{\left(1 - \tilde{r}^2\right) + 2\tilde{b}}{2(1 + 4\tilde{b})}\frac{\partial \Theta}{\partial\left(\tilde{x}/Gz\right)} = \frac{1}{\tilde{r}}\frac{\partial}{\partial\tilde{r}}\left(\tilde{r}\frac{\partial\Theta}{\partial\tilde{r}}\right), \tag{2.3}$$

with $\Theta(0, \tilde{r}) = 1$ and $\Theta(\tilde{x}, 1) = 0$.

2.2. *Nusselt number*

Using Fourier's law of thermal conduction, the local heat transfer coefficient h_x can be written as $h_x = -k/((\langle T\rangle - T_1)\,\partial_r T|_{r=R}$ (full mathematical and numerical details are given in the supplementary data available at http://dx.doi.org/10.1017/jfm.2014.733). By rewriting the temperature gradient in dimensionless form using the dimensionless flow-averaged temperature $\langle\Theta\rangle = (T_1 - \langle T\rangle)/(T_1 - T_0)$, we find for the local Nusselt number that

$$Nu_x = -\frac{2}{\langle\Theta\rangle}\left.\frac{\partial\Theta}{\partial\tilde{r}}\right|_{\tilde{r}=1}. \tag{2.4}$$

When $\tilde{x}/Gz > 0.1$, $Nu_x \to Nu_\infty$.

2.3. *Analytical expressions for thermally developing flow*

To find an analytical expression for Nu_x near the entrance of the pipe, the Lévêque approximation is followed. In that case, the governing equation can be solved in a two-dimensional Cartesian coordinate system:

$$u\frac{\partial T}{\partial x} = \alpha\frac{\partial^2 T}{\partial y^2}. \tag{2.5}$$

Here, the wall is located at $y = 0$, i.e. the direction of the y-axis is the reverse of that of the r-axis. Then, with $\tilde{y} = y/R$, the velocity profile becomes $\tilde{u} = 4(\tilde{y} + \tilde{b})/(1 + 4\tilde{b})$.

The analytical expressions for Nu_x for no-slip and no-shear flow are known (Bird *et al.* 2007). For $\tilde{b} = 0$ one can derive that

$$Nu_x = \frac{2}{9^{1/3}\Gamma\left(\frac{4}{3}\right)}\left(\frac{\tilde{x}}{Gz}\right)^{-1/3}, \tag{2.6}$$

where Γ denotes the gamma function. For no-shear flow, i.e. $b = \infty$, one finds

$$Nu_x = \frac{1}{\sqrt{\pi}}\left(\frac{\tilde{x}}{Gz}\right)^{-1/2}. \tag{2.7}$$

Thus, $\beta = 1/3$ for parabolic flow and $\beta = 1/2$ for uniform flow.

To arrive at an analytical expression for Nu_x for finite slip (i.e. $0 < \tilde{b} < \infty$), (2.5) is non-dimensionalised using $Y = y/b$ and $X = x\alpha(R+4b)/(4u_{av}b^3) = (\tilde{x}/Gz)(1+4\tilde{b})/\tilde{b}^3$. This gives

$$(1+Y)\frac{\partial\Theta}{\partial X} = \frac{\partial^2\Theta}{\partial Y^2}, \tag{2.8}$$

with $\Theta(0,Y) = 1$, $\Theta(X,0) = 0$ and $\Theta(X,\infty) = 1$. To reduce the number of variables, we perform the Laplace transformation

$$\mathscr{L}_X\left[\frac{\partial\Theta}{\partial X}\right] = \int_0^\infty \frac{\partial\Theta}{\partial X}e^{-pX}dX = p\bar{\Theta}(p,Y) - 1, \tag{2.9}$$

where $\bar{\Theta}$ is the Laplace transform of Θ. Furthermore, $\mathscr{L}_X[\partial_Y^2\Theta] = \partial_Y^2\bar{\Theta}$. The governing equation now becomes

$$(1+Y)(p\bar{\Theta} - 1) = \frac{\partial^2\bar{\Theta}}{\partial Y^2}, \tag{2.10}$$

with $\bar{\Theta}(p,0) = 0$ and $\bar{\Theta}(p,\infty) = 1/p$. Introduction of $\hat{\Theta} = \bar{\Theta} - 1/p$ and subsequent rewriting yields

$$p(1+Y)\hat{\Theta} = \frac{\partial^2\hat{\Theta}}{\partial Y^2}, \tag{2.11}$$

with $\hat{\Theta}(p,0) = -1/p$ and $\hat{\Theta}(p,\infty) = 0$. To convert this expression into an ordinary differential equation (ODE), we define $\eta = p^{1/3}(1+Y)$. Now the Airy equation is found,

$$\frac{d^2\hat{\Theta}}{d\eta^2} - \eta\hat{\Theta} = 0, \tag{2.12}$$

with $\hat{\Theta}(p^{1/3}) = -1/p$ and $\hat{\Theta}(\infty) = 0$. Its general solution of the first kind is the Airy function $Ai(\eta)$, with $\lim_{\eta\to\infty}Ai(\eta) = 0$. Then the solutions for $\hat{\Theta}$ and $\bar{\Theta}$ become

$$\hat{\Theta} = -\frac{Ai(p^{1/3}(1+Y))}{pAi(p^{1/3})} \quad \text{and} \quad \bar{\Theta} = \frac{Ai(p^{1/3}) - Ai(p^{1/3}(1+Y))}{pAi(p^{1/3})}. \tag{2.13a,b}$$

To obtain Θ, we take the inverse Laplace transform in X, giving

$$\Theta(X,Y) = \frac{1}{2\pi i}\int_{c-i\infty}^{c+i\infty}\frac{Ai(p^{1/3}) - Ai(p^{1/3}(1+Y))}{pAi(p^{1/3})}e^{pX}dp. \tag{2.14}$$

764 R3-5

For Nu_x we can derive that, given that $\langle \Theta \rangle = 1$ following the Lévêque approximation,

$$Nu_x = \frac{2}{\tilde{b}} \left. \frac{\partial \Theta}{\partial Y} \right|_{Y=0}. \tag{2.15}$$

Then, finally, we obtain

$$Nu_x = -\frac{1}{\tilde{b}\pi\mathrm{i}} \int_{c-\mathrm{i}\infty}^{c+\mathrm{i}\infty} \frac{\mathrm{Ai}'(p^{1/3})\mathrm{e}^{pX}}{p^{2/3}\mathrm{Ai}(p^{1/3})} \,\mathrm{d}p = \frac{2}{\tilde{b}} g(X). \tag{2.16}$$

The function $g(X)$ is universal, as it does not depend on $\tilde{b}$. The slip length affects the scaling between X and $\tilde{x}/Gz$, so it determines which part of the function $g(X)$ is relevant. The supplementary information provides a description of how to evaluate $g(X)$.

2.4. *Thermal and viscous boundary layer thickness*

The thermal boundary layer thickness $\tilde{\lambda}_T$ is defined as $\tilde{\lambda}_T = 1 - \tilde{r}(\Theta = 0.99)$. When $\Theta(\tilde{x}/Gz, 0) < 0.99$, $\tilde{\lambda}_T = 1$.

The viscous boundary layer $\tilde{\delta}_v$ is defined as follows. It corresponds to the point $\tilde{r} = 1 - \tilde{\delta}_v$ where the parabolic velocity component $\tilde{u}_v(\tilde{r})$ equals c times the slip velocity $\tilde{u}_s$ at the wall. Thus, $\tilde{\delta}_v(\tilde{u}_v = c\tilde{u}_s) = 1 - (1 - 2c\tilde{b})^{1/2}$. When $\tilde{b} \geqslant 1/(2c)$, $\tilde{\delta}_v = 1$. It should be noted that, for a given $\tilde{b}$ and c, $\tilde{\delta}_v$ is fixed for all $\tilde{x}/Gz$, while $\tilde{\lambda}_T = f(\tilde{x}/Gz)$.

2.5. *Numerical procedure*

Numerically, the Graetz–Nusselt problem for finite slip was solved using the pdepe solver in MATLAB (MathWorks). The relative and absolute tolerances for the pdepe solver were set at 10^{-6} and 10^{-12} respectively. To calculate $\partial_{\tilde{r}}\Theta$ at $\tilde{r} = 1$ the MATLAB function pdeval was utilised.

Because heat transport mainly occurs near the inlet and near the wall, the $\tilde{x} \times \tilde{r} = 82 \times 101$ mesh was refined near these boundaries. The exponent β was evaluated in two distinct manners. The fitting of a straight line through $\log_{10}(Nu_x)$ for $-7 \leqslant \log_{10}(\tilde{x}/Gz) \leqslant -4$ using the polyfit algorithm gives a specific constant value for β for each $\tilde{b}$, which is referred to as β_f. The gradient of $\log_{10}(Nu_x)$ or $\log_{10}(g(X))$ to $\log_{10}(\tilde{x}/Gz)$, calculated by employing the second-order-accurate gradient algorithm, gives a local value for β for each position, which is referred to as β_l. Here, Nu_∞ is taken as the average of Nu_x for $\tilde{x}/Gz \geqslant 0.1$. To compute $\langle \Theta \rangle$ the trapz script was utilised. The value of $\tilde{\lambda}_T$ was approximated by linear interpolation using the two grid points closest to $\Theta = 0.99$.

3. Results and discussion

3.1. *Nusselt profiles*

In figure 2(*a*) the Nusselt profiles are displayed for a wide range of slip lengths $\tilde{b}$. The profiles reveal that for $\tilde{b} < 10^{-4}$ the classical Graetz–Nusselt solution for no-slip flow is approached, with $\beta = 1/3$. For $\tilde{b} > 10^2$ the classical solution for no-shear flow is recovered, for which $\beta = 1/2$. For intermediate values of $\tilde{b}$, the figure shows that first the exponent β (the slope) starts to change value, followed by an increase of Nu_∞.
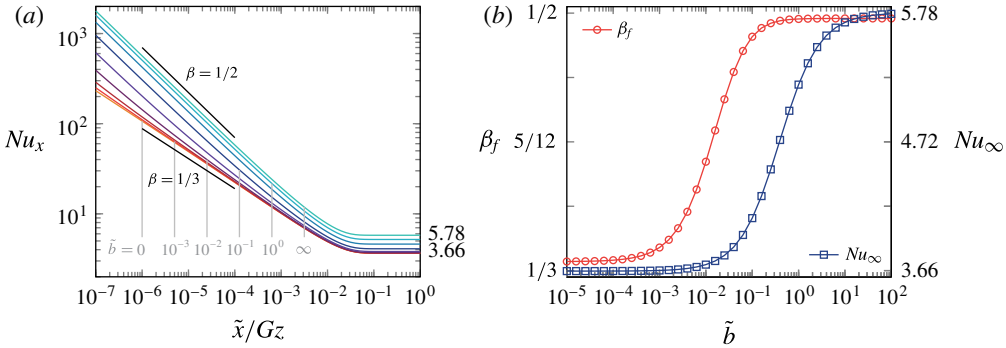
FIGURE 2. (*a*) The local Nusselt number Nu_x as a function of the position $\tilde{x}/Gz$ for various slip lengths $\tilde{b}$. The values of the scaling exponent β and the developed Nusselt number Nu_∞ for the limiting cases of no-slip ($\tilde{b} = 0$) and no-shear flow ($\tilde{b} = \infty$) are also indicated. (*b*) The scaling exponent β_f (obtained by fitting) and the developed Nusselt number Nu_∞ as a function of the slip length $\tilde{b}$. Remarkably, these two curves transition at different values of $\tilde{b}$.

The dependence of β_f and Nu_∞ on the slip length $\tilde{b}$ is shown in figure 2(*b*). This figure illustrates that the transition points for β_f and Nu_∞ are located more than one order of magnitude apart. The exponent β_f changes value when $10^{-4} < \tilde{b} < 10^0$, while Nu_∞ gradually increases from 3.66 to 5.78 when $10^{-2} < \tilde{b} < 10^2$. This corresponds to the values for Nu_∞ found by Barron *et al.* (1997), who solved the Graetz–Nusselt problem in the thermally developed regime for $0 \leqslant \tilde{b} \leqslant 0.24$ (Ezquerra Larrodé *et al.* 2000). It should be noted that a change in the range of $\tilde{x}/Gz$ values used to compute β_f results in a different transition point for β_f. The use of larger values shifts the transition point upwards. Nonetheless, the distance between the transition points for β_f and Nu_∞ remains of at least one order of magnitude.

The exponent β is not necessarily a specific constant value for finite slip as it is for no-slip and no-shear flow. Therefore, the local exponent β_l was evaluated both numerically and analytically. In figure 3(*a*), β_l is plotted versus $\tilde{x}/Gz$ for various slip lengths $\tilde{b}$. The profiles confirm that for approximately $10^{-4} < \tilde{b} < 10^0$, β_l is not constant and depends on both the position and the slip length. Furthermore, we observe that β_l always transitions from 1/2 to 1/3, except for the limits $\tilde{b} = 0$ and $\tilde{b} = \infty$.

The numerical and analytical results are in good agreement, but start to deviate when $\tilde{x}/Gz > 10^{-5}$. In that case the thermal and viscous boundary layer thicknesses are of the same order of magnitude ($\tilde{\lambda}_T \approx 0.1$ for $\tilde{x}/Gz = 10^{-4}$). Consequently, the assumptions arising from the Lévêque approximation, and therefore also the analytical results, are no longer entirely valid.

3.2. *On β and its transition point*

That β_l must transition from 1/2 to 1/3, except for $\tilde{b} = 0$ and $\tilde{b} = \infty$, can be demonstrated by inspection of the function $g(X)$. First, as figure 3(*b*) reveals, the classical limits are recovered by this function, as $Nu_x \propto g(X)$. When $\tilde{b} \to 0$, we would
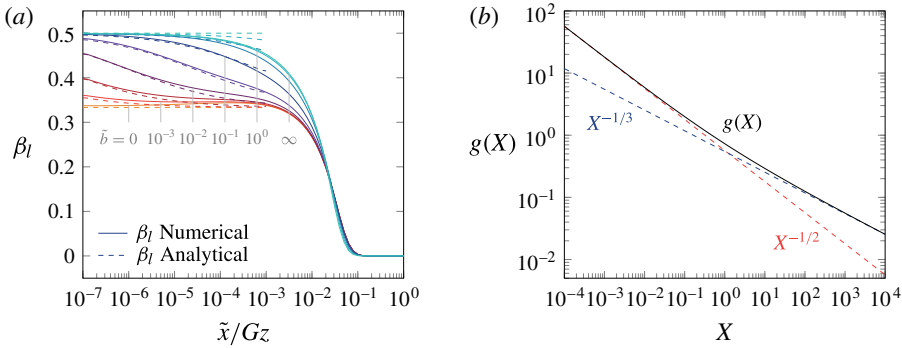
FIGURE 3. (a) The local scaling exponent β_l versus the position $\tilde{x}/Gz$ for various slip lengths $\tilde{b}$. (b) The limiting behaviour of $g(X)$, from which β_l can be obtained analytically, is as expected: $g(X) \propto X^{-1/2}$ when $X \to 0$, and $g(X) \propto X^{-1/3}$ when $X \to \infty$.

expect that $g(X) \propto X^{-1/3}$ for $X \to \infty$. Thus,

$$Nu_x \propto \frac{1}{\tilde{b}} \left(\frac{\tilde{x}}{Gz} \frac{1}{\tilde{b}^3} \right)^{-1/3} = \left(\frac{\tilde{x}}{Gz} \right)^{-1/3}. \tag{3.1}$$

When $\tilde{b} \to \infty$, we would expect that for $X \to 0$, $g(X) \propto X^{-1/2}$. Then,

$$Nu_x \propto \frac{1}{\tilde{b}} \left(\frac{\tilde{x}}{Gz} \frac{\tilde{b}}{\tilde{b}^3} \right)^{-1/2} = \left(\frac{\tilde{x}}{Gz} \right)^{-1/2}. \tag{3.2}$$

Second, for each value of $0 < \tilde{b} < \infty$ we can choose $\tilde{x}$ such that $X \to 0$. As in that case (3.2) is recovered, we find that for finite slip β_l always transitions from $1/2$ to $1/3$. Consequently, it can be concluded that for a given slip length $\tilde{b}$, the Nusselt profile in the thermally developing regime cannot be characterised by a single β_f value. The range of $\tilde{x}/Gz$ values used for computing β_f is determinant for the value of β_f that is obtained. Nevertheless, comparison of figures 2(b) and 3(a) shows that β_f does reflect for what range of slip lengths $\tilde{b}$ the exponent β changes value. Finally, since $\beta_l \approx 5/12$ when $X = 1$, the dimensionless number $X = (\tilde{x}/Gz)(1 + 4\tilde{b})/\tilde{b}^3$ can be considered as a kind of criterion for the behaviour of β: $\beta \to 1/2$ when $X \ll 1$, whereas $\beta \to 1/3$ when $X \gg 1$.

Physically, the location of the transition regime for β_l can be explained by considering the thickness of the thermal and viscous boundary layers. This is illustrated in figure 4(a). All heat transport takes place in the thermal boundary layer, where the temperature gradient at the wall, $\partial_{\tilde{r}} \Theta|_{\tilde{r}=1}$, is most important. When the velocity in the thermal boundary layer, which is growing with $\tilde{x}$, is dominated by the slip velocity $\tilde{u}_s$, $\beta_l \to 1/2$. In that case, the velocity profile in the thermal boundary layer is approximately uniform, and thereby resembles a no-shear flow. Then, the left-hand side of (2.5) can be approximated as $u\partial_x T = u_v \partial_x T + u_s \partial_x T \approx u_s \partial_x T$. On the other hand, when the velocity in the thermal boundary layer is dominated by the parabolic velocity component $\tilde{u}_v$, $\beta_l \to 1/3$. The flow profile in the thermal boundary layer resembles a no-slip flow, i.e. $u\partial_x T \approx u_v \partial_x T$, for which $\beta = 1/3$.
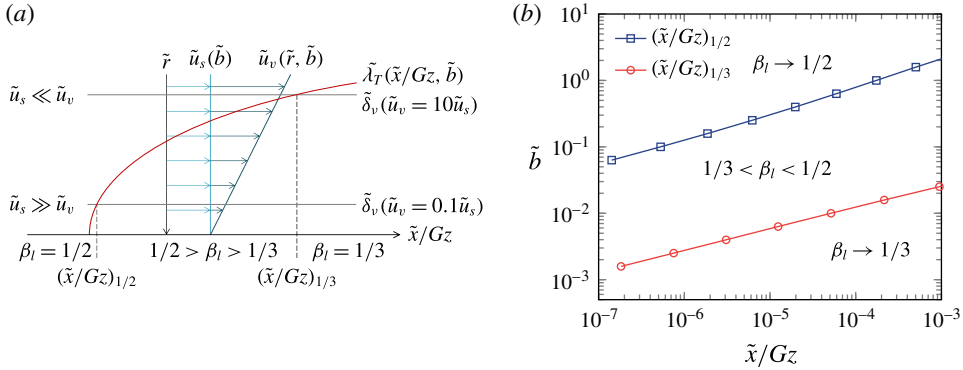
764 R3-8

FIGURE 4. (*a*) The location of the transition regime for β_l can be explained physically by considering $\tilde{\lambda}_T$ and $\tilde{\delta}_v$. When the slip velocity $\tilde{u}_s$ dominates in the thermal boundary layer, which is the case when $\tilde{x}/Gz < (\tilde{x}/Gz)_{1/2}$, $\beta_l \to 1/2$. When the velocity in the thermal boundary layer is dominated by $\tilde{u}_v$, $\beta_l \to 1/3$. This is true when $\tilde{x}/Gz > (\tilde{x}/Gz)_{1/3}$. (*b*) The locations of $(\tilde{x}/Gz)_{1/2}$ and $(\tilde{x}/Gz)_{1/3}$ as a function of the slip length $\tilde{b}$ are shown here. These points are estimated by saying that $\tilde{u}_v \ll \tilde{u}_s$ when $\tilde{u}_v = 0.1\tilde{u}_s$, and that $\tilde{u}_v \gg \tilde{u}_s$ when $\tilde{u}_v = 10\tilde{u}_s$.

The location where β_l transitions from $1/2$ to $1/3$ can be predicted. In the thermal boundary layer, the slip velocity $\tilde{u}_s$ is dominating (i.e. $\tilde{u}_v \ll \tilde{u}_s$) until the point $(\tilde{x}/Gz)_{1/2}$. This location is estimated by calculating where $\tilde{\lambda}_T = \tilde{\delta}_v(\tilde{u}_v = 0.1\tilde{u}_s)$. The parabolic velocity component starts to dominate in the thermal boundary layer (i.e. $\tilde{u}_v \gg \tilde{u}_s$) from the point $(\tilde{x}/Gz)_{1/3}$ on. The point where $\tilde{\lambda}_T = \tilde{\delta}_v(\tilde{u}_v = 10\tilde{u}_s)$ roughly corresponds to this location. This implies that the transition regime for β_l is located between $(\tilde{x}/Gz)_{1/2}$ and $(\tilde{x}/Gz)_{1/3}$. The locations of $(\tilde{x}/Gz)_{1/2}$ and $(\tilde{x}/Gz)_{1/3}$ are given in figure 4(*b*). As an example, for $\tilde{b} = 10^{-1}$ we find that $(\tilde{x}/Gz)_{1/2} = 5 \times 10^{-7}$. This is in agreement with β_l for $\tilde{b} = 10^{-1}$ in figure 3(*a*).

3.3. *On Nu_∞ and its transition point*

The developed Nusselt number Nu_∞ concerns heat transfer in the thermally developed regime ($\tilde{x}/Gz > 0.1$). In this regime the temperature and temperature gradient at the wall are approaching zero. This implies that Nu_∞ can only be enhanced by increasing advective transport near the wall, where the temperature gradients are largest. Figure 5 demonstrates that when $\tilde{u}_s$ starts to change significantly with $\tilde{b}$, Nu_∞ also transitions from 3.66 to 5.78, the limiting values for zero and infinite slip length.

Replacement of $\tilde{u}_s$ by the velocity gradient at the wall, $\partial_{\tilde{r}}\tilde{u}|_{\tilde{r}=1}$, leads to the same conclusion, however. An increase in $\tilde{u}_s$ implies that $|\partial_{\tilde{r}}\tilde{u}|$ must decrease. This follows from Navier's slip condition, $\tilde{u}_s = -\tilde{b}\,\partial_{\tilde{r}}\tilde{u}|_{\tilde{r}=1}$, which shows that the slip velocity and the velocity gradient at the wall are directly related to each other via the factor $-\tilde{b}$. Moreover, from the definitions of $\tilde{u}_s = 4\tilde{b}/(1 + 4\tilde{b})$ and $\partial_{\tilde{r}}\tilde{u}|_{\tilde{r}=1} = -4/(1 + 4\tilde{b})$, we find that they have the same transition point, which is $\tilde{b} = 1/4$. This is close to the transition point of $\tilde{b} = 0.4$ for Nu_∞. Furthermore, their derivatives to $\tilde{b}$, $\partial_{\tilde{b}}\tilde{u}_s$ and $\partial_{\tilde{b}}(\partial_{\tilde{r}}\tilde{u})|_{\tilde{r}=1}$, are both proportional to $(1 + 4\tilde{b})^{-2}$.
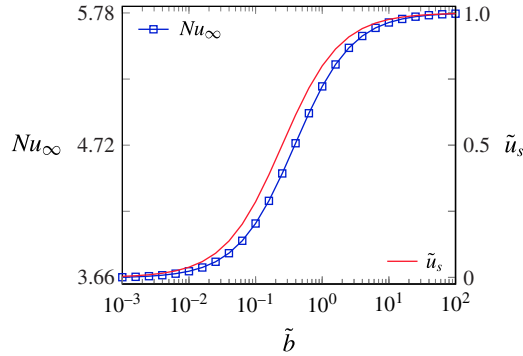
764 R3-9

FIGURE 5. The developed Nusselt number Nu_∞ and slip velocity $\tilde{u}_s$ versus the slip length $\tilde{b}$.

Therefore, the change of neither $\tilde{u}_s$ nor $\partial_{\tilde{r}}\tilde{u}|_{\tilde{r}=1}$ with slip length $\tilde{b}$ fully explains the dependence of Nu_∞ on $\tilde{b}$. It is the relation between the velocity distribution and the slip length $\tilde{b}$ that explains how Nu_∞ depends on $\tilde{b}$. Nevertheless, because heat transport is largest when temperature gradients are maximum, the change of $\tilde{u}_s$ with $\tilde{b}$ most dominantly affects the behaviour of Nu_∞. This is in agreement with the observation of Barrow & Humphreys (1970) that, given an average fluid velocity, increase of the velocity at the wall leads to larger Nusselt numbers.

3.4. *Employing wall slip to increase heat transfer*

The Nusselt profiles in figure 2(*a*) suggest that heat transport can be optimised by employing wall slip, provided that the wall slip is large enough. Partial slip lengths are usually of the order of tens of nanometres for microscale systems (Rothstein 2010). As a consequence, the maximum tube radius is approximately 1 µm for β to be significantly larger than 1/3. For Nu_∞ to be larger than 3.66, tube radii should be of the order of nanometres. However, the Graetz number is usually very small. For a typical liquid like water, $Re \sim 1$ and $Pr \sim 1$. For both micro- and nanofluidics it is estimated that $D/L < 10^{-3}$, implying that $Gz < 10^{-3}$. In that case, the temperature profile is almost instantaneously thermally developed, as this is then true for $\tilde{x} > 10^{-4}$.

Thus, enhancement of heat transfer by employing finite slip, while avoiding reaching the thermally developed regime, is possible if two conditions are met. First, the system should be designed such that $Gz > 1$. Second, the slip length should be of the order of the tube radius, i.e. $\tilde{b} \sim 1$. These conditions oppose one another. In nanofluidic systems, slip lengths $\tilde{b}$ of approximately 10^3 can be obtained (Whitby & Quirke 2007; Majumder *et al.* 2011). This implies that $\tilde{b}$ is large enough to let $Nu_\infty \to 5.78$, albeit the thermally developing section is negligibly small. Additionally, for instance, highly slippery liquid-infused porous surfaces (Lafuma & Quéré 2011; Wong *et al.* 2011) could be exploited to enhance heat transport.

It should be noted that the results presented here are applicable to systems that display homogeneous wall slip. Distinct results are expected for systems concerning effective slip (Maynes, Webb & Davies 2008; Maynes *et al.* 2012; Enright *et al.* 2013). As such, the Graetz–Nusselt problem for heterogeneously slippery surfaces deserves to be studied separately.

4. Conclusion

This study provides numerical and analytical solutions to the Graetz–Nusselt problem for continuum flows with finite slip. The classical solutions to this problem concern no-slip and no-shear flow. These form the lower and upper limits of the solutions for partial slip, as the resulting Nusselt profiles gradually transition between these limits on increasing the wall slip from zero to infinity.

The heat transfer mechanism in the thermally developing regime depends on the velocity profile in the thermal boundary layer, and is a function of wall slip and position. The ratio of the parabolic velocity component to the slip velocity determines whether it resembles the transport mechanism for no-slip or for no-shear flow. The Nusselt number in the thermally developed regime depends on the fluid velocity profile only.

By considering slip lengths ranging from zero to infinity, this study is the first to connect the classical solutions to the Graetz–Nusselt problem. This is not only of fundamental interest, but also makes it possible to evaluate the influence of wall slip on heat transfer in many forced convection problems in science and engineering.

Supplementary data

Supplementary data is available at http://dx.doi.org/10.1017/jfm.2014.733.

References

BARRON, R. F., WANG, X., AMEEL, T. A. & WARRINGTON, R. O. 1997 The Graetz problem extended to slip-flow. *Intl J. Heat Mass Transfer* **40** (8), 1817–1823.

BARROW, H. & HUMPHREYS, J. F. 1970 The effect of velocity distribution on forced convection laminar flow heat transfer in a pipe at constant wall temperature. *Wärme Stoffübertrag.* **3** (4), 227–231.

BIRD, R. B., STEWART, W. E. & LIGHTFOOT, E. N. 2007 *Transport Phenomena*, 2nd edn. John Wiley & Sons.

BOCQUET, L. & BARRAT, J.-L. 2007 Flow boundary conditions from nano- to micro-scales. *Soft Matt.* **3**, 685–693.

COLIN, S. 2011 Gas microflows in the slip flow regime: a critical review on convective heat transfer. *J. Heat Transfer* **134** (2), 020908.

ECKERT, E. R. G. & DRAKE, R. M. 1972 *Analysis of Heat and Mass Transfer*. McGraw-Hill.

ENRIGHT, R., HODES, M., SALAMON, T. & MUZYCHKA, Y. 2013 Isoflux Nusselt number and slip length formulae for superhydrophobic microchannels. *J. Heat Transfer* **136** (1), 012402. doi:10.1115/1.4024837.

EZQUERRA LARRODÉ, F., HOUSIADAS, C. & DROSSINOS, Y. 2000 Slip-flow heat transfer in circular tubes. *Intl J. Heat Mass Transfer* **43** (15), 2669–2680.

GRAETZ, L. 1882 Über die Wärmeleitungsfähigkeit von Flüssigkeiten. *Ann. Phys.* **254** (1), 79–94.

GRAETZ, L. 1885 Über die Wärmeleitungsfähigkeit von Flüssigkeiten. *Ann. Phys.* **261** (7), 337–357.

JAKOB, M. 1949 *Heat Transfer,* vol. 1. John Wiley & Sons.

KARNIADAKIS, G., BESKOK, A. & ALURU, N. 2005 *Microflows and Nanoflows: Fundamentals and Simulation*. Springer.

LAFUMA, A. & QUÉRÉ, D. 2011 Slippery pre-suffused surfaces. *Europhys. Lett.* **96** (5), 56001.

LAUGA, E., BRENNER, M. P. & STONE, H. A. 2007 Microfluidics: the no-slip boundary condition. In *Springer Handbook of Experimental Fluid Mechanics* (ed. C. Tropea, A. L. Yarin & J. F. Foss), pp. 1219–1240. Springer.

LÉVÊQUE, M. A. 1928 Les lois de la transmission de chaleur par convection. *Ann. Mines, Mem., Ser.* **13** (12), 201–299, 305–362, 381–415.

MAJUMDER, M., CHOPRA, N. & HINDS, B. J. 2011 Mass transport through carbon nanotube membranes in three different regimes: ionic diffusion and gas and liquid flow. *ACS Nano* **5** (5), 3867–3877.

MAYNES, D., WEBB, B. W. & DAVIES, J. 2008 Thermal transport in a microchannel exhibiting ultrahydrophobic microribs maintained at constant temperature. *J. Heat Transfer* **130** (2), 022402.

MAYNES, D., WEBB, B. W., CROCKETT, J. & SOLOVJOV, V. 2012 Analysis of laminar slip-flow thermal transport in microchannels with transverse rib and cavity structured superhydrophobic walls at constant heat flux. *J. Heat Transfer* **135** (2), 021701. doi:10.1115/1.4007429.

NAVIER, C. L. M. H. 1823 Mémoire sur les lois du mouvement des fluids. *Mem. Acad. Sci. Inst. Fr.* **6**, 389–416, 432–436.

NUSSELT, W. 1910 Die Abhängigkeit der Wärmeübergangszahl von der Rohrlänge. *Z. Verein. Deutsch. Ing.* **54** (28), 1154–1158.

ROTHSTEIN, J. P. 2010 Slip on superhydrophobic surfaces. *Annu. Rev. Fluid Mech.* **42** (1), 89–109.

SHAH, R. K. & LONDON, A. L. 1978 *Laminar Flow Forced Convection in Ducts: A Source Book for Compact Heat Exchanger Analytical Data*. Academic.

SPARROW, E. M. & LIN, S. H. 1962 Laminar heat transfer in tubes under slip-flow conditions. *J. Heat Transfer* **84** (4), 363–369.

WHITBY, M. & QUIRKE, N. 2007 Fluid flow in carbon nanotubes and nanopipes. *Nat. Nano* **2** (2), 87–94.

WONG, T.-S., KANG, S. H., TANG, S. K. Y., SMYTHE, E. J., HATTON, B. D., GRINTHAL, A. & AIZENBERG, J. 2011 Bioinspired self-repairing slippery surfaces with pressure-stable omniphobicity. *Nature* **477** (7365), 443–447.